

# Paramagnetic Resonance of $\text{Fe}^{3+}$ in Octahedral and Tetrahedral Sites in Yttrium Gallium Garnet (YGaG) and Anisotropy of Yttrium Iron Garnet (YIG)

S. GESCHWIND

*Bell Telephone Laboratories, Murray Hill, New Jersey*

(Received September 14, 1960)

The electron paramagnetic resonance spectrum of a small  $\text{Fe}^{3+}$  impurity which enters substitutionally for the gallium in single crystals of yttrium gallium garnet (chemical formula  $\text{Y}_3\text{Ga}_5\text{O}_{12}$ ) has been examined at 24 kMc/sec at 295°K and 1.6°K.  $\text{Fe}^{3+}$  is studied for the first time in tetrahedral coordination. The results for the crystal field parameters that appear in the usual spin Hamiltonian for  $\text{Fe}^{3+}$  for the octahedral ( $a$ ) and tetrahedral ( $d$ ) sites are:  $a_a = +0.0185 \text{ cm}^{-1}$ ,  $D_a = -0.1294 \text{ cm}^{-1}$ ,  $F_a = +0.0026 \text{ cm}^{-1}$ ,  $a_d = +0.0062 \text{ cm}^{-1}$ ,  $D_d = -0.0880 \text{ cm}^{-1}$ ,  $F_d = -0.0037 \text{ cm}^{-1}$ .

The finding of  $a$  positive in both types of sites where the cubic crystalline potential,  $V$ , has opposite signs indicates that in the mechanism responsible for this splitting terms proportional to even powers of  $V$  are dominant. Using the experimentally determined crystal field parameters of  $\text{Fe}^{3+}$  in YGaG, the low-temperature anisotropy energy per unit cell in the isostructural ferrimagnet, YIG, is predicted as  $K_1 = -0.370 \text{ cm}^{-1}$ . This is 50% larger than the experimental value  $K_1 = -0.250 \text{ cm}^{-1}$  and several sources for the origin of this discrepancy are suggested.

## I. INTRODUCTION

TRIVALENT iron is in a  $3d^5$ ,  $^6S_5$  ground state, which has no orbital angular momentum and is spherically symmetric so that it cannot be directly affected by any crystalline electric field. Nevertheless, a splitting of the ground state is familiarly observed in paramagnetic resonance experiments which is explained as arising from a small admixture to the  $^6S_5$  state of small amounts of higher multiplets and configurations which are split by the crystalline electric field. The exact nature of the mechanism of this splitting is still uncertain involving as it does higher order processes through the combined action of crystalline electric field, spin-orbit coupling and spin-spin interactions. Watanabe<sup>1</sup> has recently considered this problem in detail (the problem is the same for  $\text{Mn}^{2+}$  which has the same configuration and ground state) and concluded that any perturbation of the ground state arising from higher multiplets of the  $3d^5$  configuration involve the crystalline potential,  $V$ , to even powers only and will first appear as  $(V^2)$ . Perturbations from higher configurations such as  $3d^44s$  can involve  $V$  to the first power but for cubic crystalline fields are generally expected to be less than one-tenth as effective due to their greater separation from the ground state.

More recently, Powell, Gabriel, and Johnston<sup>2</sup> have criticized Watanabe's results and have performed a detailed calculation of the ground state splitting showing that contributions to this splitting which are odd in  $V$  arise from terms in  $d^5$ . The sign of the coefficient  $C$  in the cubic crystalline potential,

$$V = C(x^4 + y^4 + z^4 - \frac{2}{3}r^4), \quad (1)$$

at the center of an octahedron of point charges is

opposite to the sign of  $C$  at the center of a tetrahedron of point charges of the same polarity. If the sign of the ground-state splitting parameters,  $a$ , is found to be the same for an ion in both types of coordination, then one can at least conclude that terms even in  $V$  are still dominant.

This point has already been verified for  $\text{Mn}^{2+}$  by Watkins<sup>3</sup> who found a positive sign for  $a$  for  $\text{Mn}^{2+}$  in ZnS and for  $\text{Mn}^{2+}$  in germanium (which too is in a  $^6S_5$  ground state), i.e., both cases of tetrahedral coordination, while a positive sign for  $a$  is also found for  $\text{Mn}^{2+}$  in octahedral coordination.<sup>4,5</sup>

In yttrium gallium garnet (chemical formula  $\text{Y}_3\text{Ga}_5\text{O}_{12}$ , hereinafter called YGaG) the small Fe impurity enters substitutionally as  $\text{Fe}^{3+}$  for the Ga in both octahedral and tetrahedral sites at whose vertices are found  $\text{O}^{2-}$  ions. This affords us the opportunity to study for the first time the paramagnetic resonance spectrum of  $\text{Fe}^{3+}$  in tetrahedral coordination and thereby to check that aspect of the theory which predicts that the sign of  $a$  is essentially independent of the sign of  $V$ .

The second area of interest is the bearing of this observed cubic crystalline field anisotropy of  $\text{Fe}^{3+}$  upon the anisotropy of cubic ferrimagnetic crystals with  $S$ -state ions such as the ferrites and ferrimagnetic garnets. Until recently, the origin of the magnetocrystalline anisotropy of cubic ferrimagnetic substances remained a puzzle. It seemed that the several types of energy terms that are present in a ferrimagnet should not contribute to a magnetocrystalline anisotropy energy. For example, the exchange energy  $-JS_i \cdot S_j$  is isotropic and should not depend upon the orientation of the spin system relative to the crystal axes. The

<sup>1</sup> H. Watanabe, Progr. Theoret. Phys. (Kyoto) **18**, 405 (1957).

<sup>2</sup> M. J. D. Powell, J. R. Gabriel, and D. F. Johnston, Phys. Rev. Letters **5**, 145 (1960). The author is indebted to W. M. Walsh, Jr. for calling this work to his attention in preprint form.

<sup>3</sup> G. D. Watkins, Phys. Rev. **110**, 986 (1958); Bull. Am. Phys. Soc. **2**, 345 (1957).

<sup>4</sup> B. Bleaney and D. J. E. Ingram, Proc. Roy. Soc. (London) **A205**, 335 (1951).

<sup>5</sup> W. Low, Phys. Rev. **105**, 792 (1957).

magnetic dipole energy,

$$\frac{\mathbf{S}_i \cdot \mathbf{S}_j}{r_{ij}^3} - \frac{3(\mathbf{S}_i \cdot \mathbf{r}_{ij})(\mathbf{S}_j \cdot \mathbf{r}_{ij})}{r_{ij}^5},$$

does contain an anisotropic term but this term can be shown classically to average to zero in a cubic crystal.<sup>6,7</sup> While, as Van Vleck has shown,<sup>6</sup> in a quantum mechanical treatment of the magnetic dipole energy of a cubic lattice, higher order effects contribute to the anisotropy, Yosida and Tachiki<sup>8</sup> have shown that this can account for only approximately 10% of the observed anisotropy. A third mechanism is the anisotropic exchange interaction which is produced by the combined action of spin-orbit coupling and the exchange interaction.<sup>6</sup> Here again calculation by Yosida and Tachiki<sup>8</sup> shows that the contribution from this source is far too small to account for the observed anisotropy. However, it was recognized almost concurrently by Yosida and Tachiki,<sup>8</sup> Wolf<sup>9</sup> and Rado and Folen<sup>10,11</sup> that the observed anisotropy of ferrimagnets was of the same order of magnitude as the anisotropy of the  $\text{Fe}^{3+}$  ion in cubic crystal fields as seen in paramagnetic resonance. This led them to propose that the anisotropy does not arise from interactions between the magnetic ions but is rather a single ion property and it is this single ion crystal field anisotropy averaged over the different sites of the crystal which gives the observed ferrimagnetic anisotropy. A fairly direct experimental check of this thesis would be to do paramagnetic resonance in a diamagnetic crystal which is isomorphous with the ferrimagnetic crystal and which is doped with a small amount of the paramagnetic ions found in the ferrimagnetic crystal. One is then presumably determining the crystal field splitting parameters in a crystalline field environment that is almost identical to the ferrimagnetic crystal. YGaG doped with a small  $\text{Fe}^{3+}$  impurity is a very good test sample as it is isomorphous with the very important yttrium iron garnet (YIG). In Sec. II a description of the experimental equipment will be given. This will be followed by the experimental results in Sec. III. In Sec. IV the measured crystal field parameters of the spin Hamiltonian will be compared with Watanabe's theory and in Sec. V these parameters will be related to the measured anisotropy of YIG.

## II. EXPERIMENTAL PROCEDURE

Single crystals of yttrium gallium garnet doped with iron were grown from the melt by J. W. Remeika and J. W. Neilsen of these laboratories. All samples contained less than 0.1% Fe which entered substitutionally

as  $\text{Fe}^{3+}$  for the gallium in the octahedral and tetrahedral sites. That it did indeed enter substitutionally is implicit in the paramagnetic resonance spectra observed and the known site symmetries. However, a random distribution of  $\text{Fe}^{3+}$  between octahedral and tetrahedral sites was not obtained; instead it was found that approximately ten times as much iron lodged in octahedral sites. Several efforts to obtain a more nearly random distribution of the  $\text{Fe}^{3+}$  between the octahedral and tetrahedral sites, by quenching the crystal from a temperature near its melting point, proved unsuccessful.<sup>12</sup> As a result, the resonance lines from the octahedral spectra often swamped those from the tetrahedral spectra and great care was needed to resolve the tetrahedral site lines.

The paramagnetic resonance spectrometer was of the balanced microwave bridge type with superheterodyne detection and is shown schematically in Fig. 1. Single crystals weighing approximately 30 milligrams were oriented on polystyrene rods so that in one case the rod axis coincided with a  $[110]$ , while in another with a  $[100]$  direction. The specimen was contained in a 24-kMc/sec  $TE_{0,1,n}$  circular cavity with the rod axis at right angles to the plane of the dc magnetic field. The magnet could be rotated about a vertical direction so that the magnetic field could be rotated in the  $[110]$  or  $[100]$  planes for the two different mountings. One arm of the bridge contained the microwave reflection type cavity, while the other contained a phase shifter and attenuator used to balance the bridge for zero microwave output off resonance. The reflection type cavity was equipped with a variable matching device suggested by R. Kompfner and first put into practice by J. P. Gordon of this laboratory.<sup>13</sup> This matching device used a short section of variable-length waveguide beyond cut-off to couple to the normally overcoupled cavity. With a matched cavity in one arm, the attenuator in the other arm was usually set for maximum attenuation and was only occasionally used along with the phase shifter to cancel any residual reflections from the cavity arm. From the point of view of microphonic noise, the perfectly matched reflection type cavity seems most desirable. In this way both arms of the bridge are matched. Microphonics originating in vibration of the waveguide arm leading to the cavity and the balancing arm of the bridge are generally phase modulations whose effect in unbalancing the bridge will be minimal if the reflections from each arm are minimized. While looking at the absorption signal minimizes such phase unbalance effects, they are further reduced by working with matched arms.

In the initial stages of the work at room temperature, the 2K50 signal klystron was locked on the microwave cavity containing the specimen by using a Pound dc

<sup>6</sup> J. H. Van Vleck, *Phys. Rev.* **52**, 1178 (1937).

<sup>7</sup> J. I. Kaplan, *J. Chem. Phys.* **22**, 1709 (1954).

<sup>8</sup> K. Yosida and M. Tachiki, *Progr. Theoret. Phys. (Kyoto)* **17**, 331 (1957).

<sup>9</sup> W. Wolf, *Phys. Rev.* **108**, 1152 (1957).

<sup>10</sup> G. T. Rado and V. J. Folen, *Bull. Am. Phys. Soc.* **1**, 132 (1956).

<sup>11</sup> V. J. Folen and G. T. Rado, *J. Appl. Phys.* **29**, 438 (1958).

<sup>12</sup> D. Linn, Bell Telephone Laboratories (unpublished memorandum).

<sup>13</sup> J. P. Gordon (private communication).



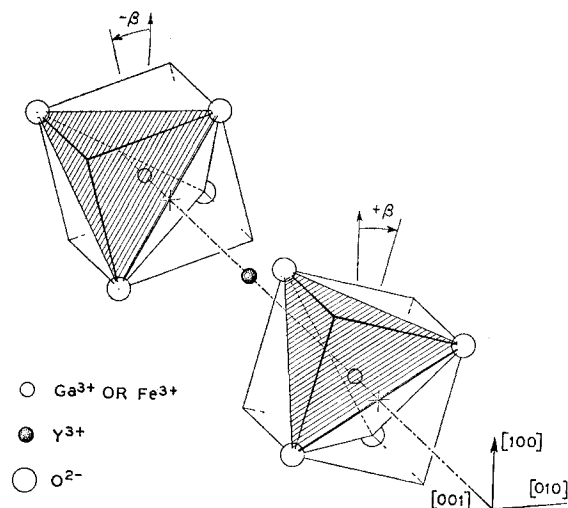


FIG. 2. The positions of the tetrahedra may be visualized by starting with regular tetrahedra inscribed in a cube whose axes are coincident with the unit cell edges. The cube is then stretched along a unit cell edge,  $\langle 001 \rangle$  and then rotated about this axis through opposite angles  $\beta$  giving rise to two types of sites for this common axis of distortion.

Here  $D$  and  $F$  correspond to axial fields of the second and fourth degree, respectively, with the  $z$  axis chosen along the direction of the axial crystal field.  $a$  is the cubic crystal field splitting parameter and  $\xi, \eta, \zeta$  are the axes of the cubic crystalline fields, none of which, in general, need coincide with the  $z$  axis. Each octahedron is distorted by a stretching along one of its threefold axes and has site symmetry  $C_{3i}$  with the trigonal axes coinciding with one of the  $[111]$  directions of the crystal.

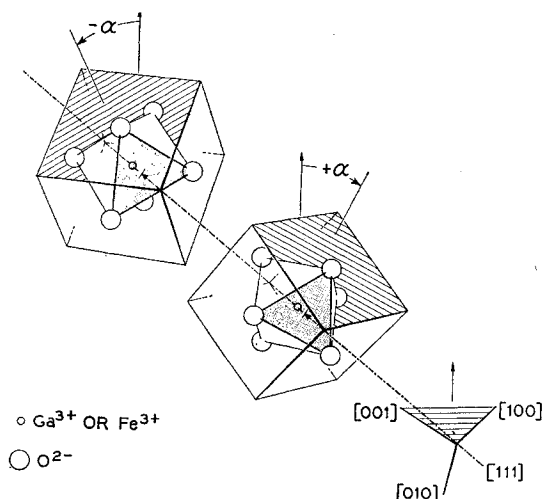


FIG. 3. Two nonequivalent octahedral sites can be associated with each of the  $\langle 111 \rangle$  axes. The position of these octahedra may be visualized by starting from a pair of regular octahedra inscribed in cubes whose edges are parallel to the crystal axes,  $\langle 100 \rangle$ . The octahedra are first distorted by stretching along a  $\langle 111 \rangle$  direction. They are then rotated about this crystal  $\langle 111 \rangle$  direction through opposite angles  $\alpha$ . These are the sites  $(a_1)$  and  $(a_2)$  described in the text.

The tetrahedra are distorted by a pulling along one of their fourfold rotary-inversion axes and have site symmetry  $S_4$ , with the tetragonal axes along any one of the  $[100]$  directions of the crystal. The axial distortions are fairly severe and give rise to an axial term in the spin Hamiltonian for each site which is considerably larger than the cubic term. Even among those sites having a common axis of distortion there are two types which are distinguished from each other by a rotation in opposite directions about the axis. (See Figs. 2 and 3.) Thus there are 14 nonequivalent sites for the  $\text{Fe}^{3+}$  impurity as far as crystal field orientation is concerned. With the magnetic field in a general direction, this will give rise to 70 lines, corresponding to  $\Delta S_z = \pm 1$  transitions, five for each nonequivalent site. The situation is simplified, however, by confining the magnetic field to a principal plane such as a  $(110)$  or  $(100)$ , and even further

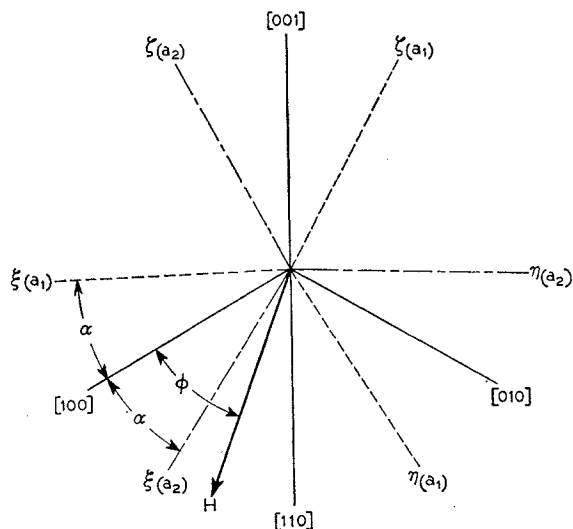


FIG. 4. Projection onto the  $(111)$  plane of the cubic crystal field axes of the octahedra, the unit-cell edges and the external magnetic field. All angles are measured in the  $(111)$  plane.

simplification results with the magnetic field along a  $[100]$  or  $[111]$  direction.

It is convenient to rewrite the spin Hamiltonian relative to a set of axes which more specifically express the point symmetry of the octahedral and tetrahedral sites.

Octahedral site ( $C_{3i}$ ):

$$\begin{aligned} \mathcal{H} = & g\beta H S_z \cos\theta + \frac{1}{2} g\beta H \sin\theta (S_+ + S_-) \\ & + D[S_z^2 - \frac{1}{3} S(S+1)] \\ & - (1/180)(a-F)\{35S_z^4 - 30S(S+1)S_z^2 + 25S_z^2 \\ & - 6S(S+1) + 3S^2(S+1)^2\} \\ & + (a\sqrt{2}/36)[S_+^3 e^{i\beta(\varphi \mp \alpha)} + S_-^3 e^{-i\beta(\varphi \mp \alpha)} \\ & + (S_+^3 e^{i\beta(\varphi \mp \alpha)} + S_-^3 e^{-i\beta(\varphi \mp \alpha)})S_z]. \quad (3) \end{aligned}$$

Here, as before, the  $z$  axis is along the axis of distortion of the octahedron (a  $\langle 111 \rangle$  direction), and the  $x$  axis is chosen to coincide with the projection of  $H$  upon a plane

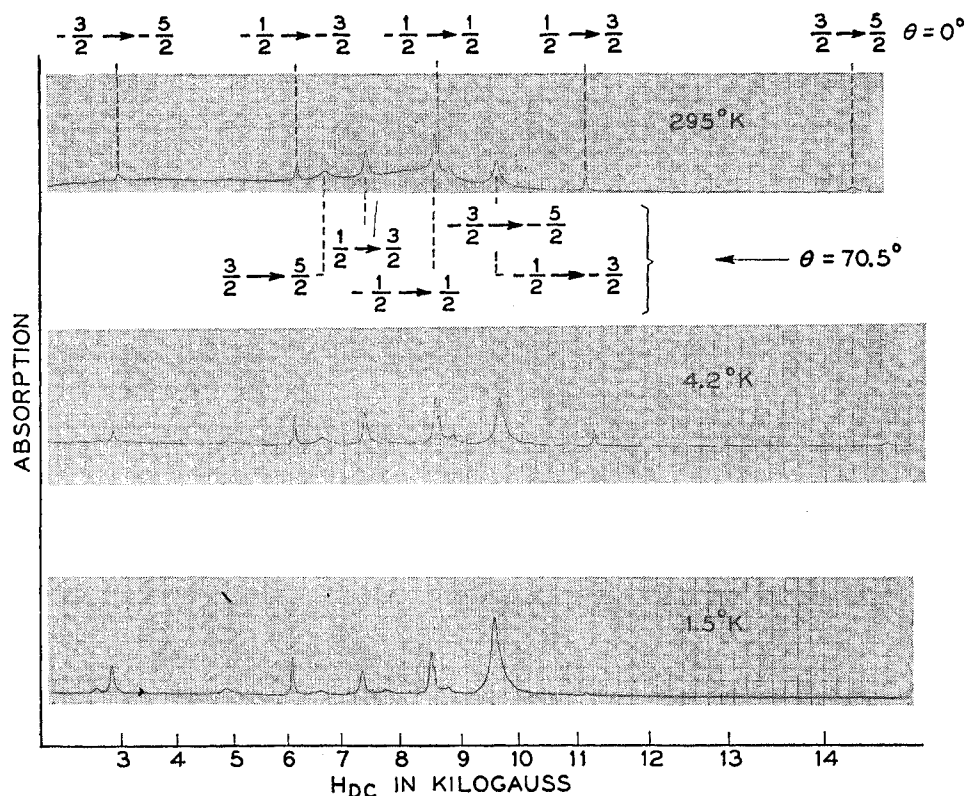


FIG. 5. Spectra observed with the magnetic field along a  $[111]$  direction. There are two octahedral spectra, one corresponding to  $\theta=0^\circ$  and three coincident spectra at  $\theta=70.5^\circ$  corresponding to the angle between  $H_{d0}$  and the other three body diagonals.

perpendicular to  $z$ .  $\theta$  is the angle between  $H$  and  $z$ .  $S_+ = S_x + iS_y$  and  $S_- = S_x - iS_y$ . The remaining angles are illustrated in Fig. 4.  $\alpha$  is the angle through which the octahedra are rotated about the  $z$  axis, away from the position where the cubic crystal field axes would coincide with the unit-cell edges.  $\varphi$  is the angle between  $H_1$  and the projection of one of the unit-cell edges onto the  $(111)$  plane. The  $\mp\alpha$  distinguish between the two types of sites ( $a_1$ ) and ( $a_2$ ) rotated from each other by  $2\alpha$  about a common  $z$  axis.

Tetrahedral site ( $S_4$ ):

$$\begin{aligned} 3\mathcal{C} = & g\beta HS_z \cos\theta + \frac{1}{2}g\beta H \sin\theta(S_+ + S_-) \\ & + D[S_z^2 - \frac{1}{3}S(S+1)] \\ & + (1/120)(a + \frac{2}{3}F)[35S_z^4 - 30S(S+1)S_z^2 \\ & + 25S_z^2 - 6S(S+1) + 3S^2(S+1)^2] \\ & + (a/48)[S_+^4 e^{i4(\varphi \pm \beta)} + S_-^4 e^{-i4(\varphi \pm \beta)}]. \quad (4) \end{aligned}$$

Here  $\varphi$  is the angle between  $H_1$  and the unit-cell edges and  $\beta$  is the angle of rotation of the cubic axes of the tetrahedra about their  $z$  axes away from the position where their cubic crystal field axes would coincide with the unit-cell edges. (See Fig. 2.)

With the magnetic field parallel to the  $z$  axis (parallel spectrum) the Hamiltonian is diagonal except for the azimuthal terms in powers of  $S_+$  and  $S_-$  which in our case amount to a small second order correction. In this case, the fields for resonance at fixed microwave fre-

quency corresponding to the  $\Delta S_z = \pm 1$  transitions are given by the following expressions:

Octahedral Sites

$$\begin{aligned} \pm \frac{3}{2} \rightarrow \pm \frac{5}{2}: H_{1,5} &= H_0 \mp 4D \pm \frac{4}{3}(a-F) - \frac{20}{27} \frac{a^2}{H_{1,5} \pm 2D}, \\ \pm \frac{1}{2} \rightarrow \pm \frac{3}{2}: H_{2,4} &= H_0 \mp 2D \mp \frac{5}{3}(a-F) + \frac{20}{27} \frac{a^2}{H_{2,4} \mp 2D}, \quad (5) \\ -\frac{1}{2} \rightarrow +\frac{1}{2}: H_3 &= H_0 - \frac{20}{27} a^2 \left( \frac{1}{H_3 + 2D} + \frac{1}{H_3 - 2D} \right). \end{aligned}$$

Tetrahedral Sites

$$\begin{aligned} \pm \frac{3}{2} \rightarrow \pm \frac{5}{2} &= H_{1,5} = H_0 \mp 4D \mp 2(a + \frac{2}{3}F) \\ &\quad - \frac{5}{16} a^2 \left( \frac{1}{H_{1,5} \pm D} - \frac{1}{H_{1,5} \mp D} \right), \\ \pm \frac{1}{2} \rightarrow \pm \frac{3}{2} &= H_{2,4} = H_0 \mp 2D \pm \frac{5}{2}(a + \frac{2}{3}F) \\ &\quad - \frac{5}{16} \frac{a^2}{H_{2,4} \mp D}, \quad (6) \\ -\frac{1}{2} \rightarrow +\frac{1}{2} &= H_3 = H_0, \\ H_0 &= h\nu/g\beta. \end{aligned}$$

While there are closed expressions for the resonance

TABLE I. Ground-state crystal field splitting parameters of  $\text{Fe}^{3+}$  in yttrium gallium garnet (YGaG) in  $\text{cm}^{-1}$ .

	Octahedral [(a) site]		Tetrahedral [(d) site]	
	295°K	4.2°K	295°K	4.2°K
$D$	$-0.1295 \pm 0.0003$	$-0.1320 \pm 0.0004$	$-0.0885 \pm 0.0005$	$-0.0880 \pm 0.0006$
$a$	$+0.0185 \pm 0.0003$	$+0.0189 \pm 0.0007$	$+0.0062 \pm 0.0003$	$+0.0062 \pm 0.0004$
$F$	$+0.0026 \pm 0.0004$	$+0.0034 \pm 0.0007$	$-0.0037 \pm 0.0004$	$-0.0038 \pm 0.0005$
$g$	$2.003 \pm 0.001$		$2.0047 \pm 0.0005$	

fields for the parallel spectrum, they are relatively unwieldy compared to the approximate formulas above, which have more than sufficient accuracy for our case. The fields for resonance in Eq. (5) have been given previously in this form by Kornienko and Prokhorov<sup>18</sup> for  $\text{Fe}^{3+}$  in  $\text{Al}_2\text{O}_3$ , however, we disagree in the matter of signs in several places.

In the denominators of the terms in  $a^2$ ,  $a$ , and  $F$  have been neglected compared to  $H$  and  $D$ . At 24 kMc/sec the terms in  $a^2$  amount to a very small correction and can be initially neglected. This correction can be inserted after  $a$  has been determined. Thus, from the parallel spectrum of the octahedral site  $D_a$  and  $(a_a - F_a)$  can be determined and similarly for the tetrahedral site  $D_d$  and  $(a_d + \frac{2}{3}F_d)$  can be found. Only the relative signs of  $D_a$  and  $(a_a - F_a)$  and  $D_d$  and  $(a_d + \frac{2}{3}F_d)$  can be found at room temperature, the absolute signs are determined by observation of the relative intensity of the lines at 4.2°K. The determination of  $a$  will be described in the next section.

#### IV. EXPERIMENTAL RESULTS

We initially confine our attention to the octahedral sites. With the magnetic field applied along a  $[111]$  direction one observes the five  $\Delta S_z = \pm 1$  lines corresponding to those octahedral sites whose axes of distortion lie along this particular  $[111]$  direction. These lines are labeled  $\theta = 0^\circ$  in Fig. 5. The intensity of the lines moving out from either side of center should be in the ratio 9:8:5. While the peak intensities do not follow these ratios, presumably due to crystal field broadening of the outer components, the integrated intensities are in fair agreement with these ratios. The  $z$  axes of the remaining octahedra lie along the three other  $\langle 111 \rangle$  directions and all will make angles of  $70.5^\circ$  with the applied field and their spectra will coincide. Their positions in Fig. 5 can be seen to agree with the fields for resonance,  $H_{\text{res}}$ , at  $\theta = 70.5^\circ$  in Fig. 6, where  $H_{\text{res}}$  has been plotted versus  $\theta$  with the magnetic field rotated in the  $(110)$  plane.

From this parallel spectrum  $D$  and  $(a - F)$  can be determined from Eq. (5), neglecting the second order terms, with relative signs. The increase at low temperature of the outside low-field line relative to the outside high-field line labels these transitions, respectively, as the  $-\frac{3}{2} \rightarrow -\frac{5}{2}$  and  $+\frac{3}{2} \rightarrow +\frac{5}{2}$  and establishes  $D$  as

negative. The final results are listed in Table I, where the crystal field parameters are given in  $\text{cm}^{-1}$ , and may be expressed in oersteds as is often done by multiplying by  $ch/g\beta = 2.1412 \times 10^4/g$ . Here  $c$  is the velocity of light,  $h$  is Planck's constant,  $\beta$  is the Bohr magneton, and  $g$  is the  $g$  value of the ion in question.

The other unlabeled lines which appear at low field correspond to  $\Delta S_z = \pm 2$  transitions. In addition, several other less intense lines which appear at low temperature

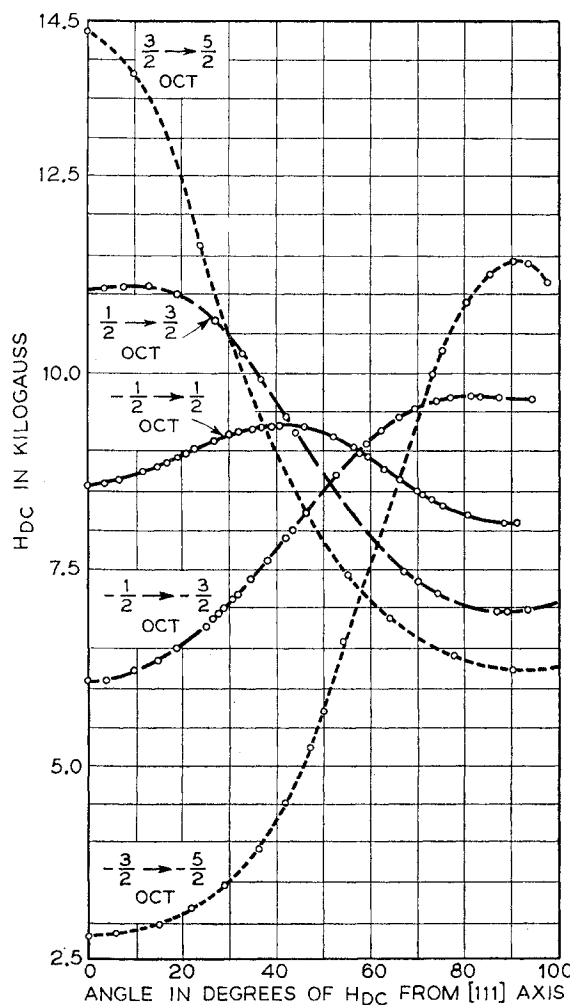
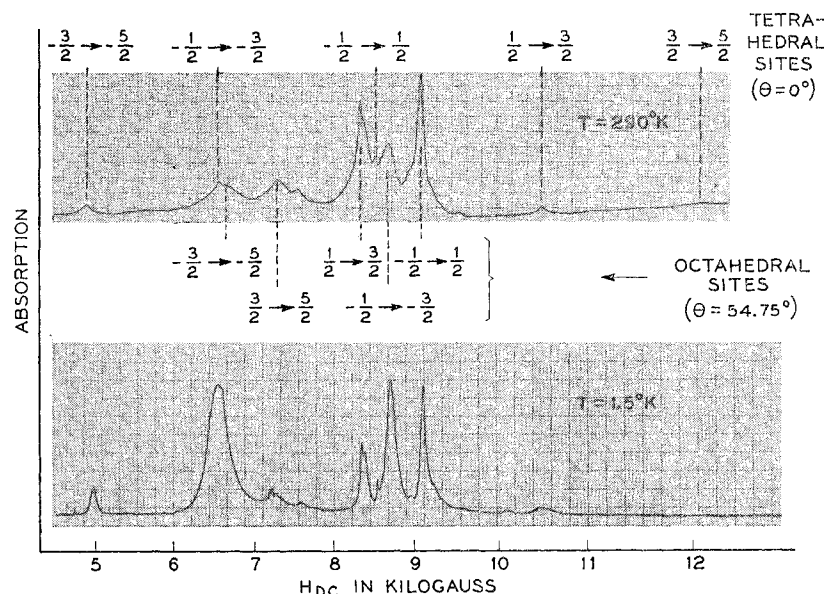


FIG. 6. Field for resonance vs  $\theta$  of the  $\Delta S_z = \pm 1$  lines for the octahedral sites distorted along the  $[111]$  direction, with the magnetic field rotated in the  $(110)$  plane. In this plane there is no  $\varphi$  splitting. Spectra from the octahedral sites distorted along the other body diagonals are not shown.

<sup>18</sup> L. S. Kornienko and A. M. Prokhorov, J. Exptl. Theoret. Phys. (U.S.S.R.) 33, 805 (1957) [translation Soviet Phys.—JETP 6(33), 620 (1958)].

FIG. 7. Spectra observed with  $H$  along a  $[100]$  direction. The sharp line riding on the  $+\frac{1}{2} \rightarrow +\frac{3}{2}$  transition of the octahedral site is composed of two coincident  $-\frac{1}{2} \rightarrow +\frac{1}{2}$ ,  $\theta=90^\circ$  lines of the tetrahedral sites.



have been tentatively identified as arising from the platinum which diffused into the melt from the platinum crucibles in which the crystals were grown.

Turning now to the tetrahedral sites, with the magnetic field along a  $[100]$  direction we will observe the five  $\Delta S_z = \pm 1$  lines of the parallel spectrum for those tetrahedral sites whose axes of distortion are along that particular  $[100]$  direction as shown in Fig. 7. The low-field ( $-\frac{3}{2} \rightarrow -\frac{5}{2}$ ) line is coincident with a  $\Delta m = 2$  transition of  $\text{Fe}^{3+}$  in the much more heavily doped ( $a$ ) sites which masks it. This recording illustrates how much less iron entered the tetrahedral sites as compared to the octahedral sites. The most prominent feature of this spectrum is still the octahedral site lines, all octahedral sites being equivalent with  $H$  along a  $[100]$  direction, their  $z$  axes making an angle of  $54.75^\circ$  with  $H$ . With  $H$  parallel to the  $[100]$  direction, one also observes the right-angle spectrum of those tetrahedral sites whose  $z$  axes lie along the  $[010]$  and  $[001]$  directions. Normally, these lines should be twice as intense as the parallel spectrum as there are twice as many sites. However, as mentioned earlier, crystal field variations due to imperfections broaden the lines away from  $\theta = 0$ . The integrated intensities of corresponding lines should still be 2:1, however, only a qualitative check of this was possible as the tetrahedral site lines were so much weaker and were often masked by the much more intense lines of the octahedral sites. This also made it difficult to follow all the tetrahedral site lines as the magnetic field was changed.

The value for  $D$  and for the tetrahedral sites is given in Table I.

#### Determination of $a$

The manner in which  $a$  was determined independently of  $F$ , for both sites, is most conveniently illustrated for

the case of the tetrahedral sites. From the Hamiltonian given in Eq. (4) it is seen that  $a$  appears independently of  $F$  as an  $ae^{i4\varphi}$  term, so that if  $H$  is varied azimuthally in such a way as to keep  $\theta$  constant then the resultant variation in the spectrum will reflect the influence of  $a$ . This was easily done by rotating  $H$  in a  $(001)$  plane and observing the  $-\frac{1}{2} \rightarrow +\frac{1}{2}$  transition. Among those tetrahedral sites having their  $z$  axes along the  $[001]$  direction there are two types, which we call  $d_1$  and  $d_2$ , distinguished from each other in that they are rotated about this  $[001]$  direction from a position where the cubic axes of the tetrahedra are coincident with the unit-cell edges, through angles  $+\beta$  and  $-\beta$ , respectively. (See Fig. 2.)

As  $H_{ac}$  is rotated in the  $(001)$  plane these two sites will give rise to two distinct spectra corresponding to the term

$$a[S_+^4 e^{i4(\varphi \pm \beta)} + S_-^4 e^{-i4(\varphi \pm \beta)}]$$

in the Hamiltonian given in Eq. (4). This is illustrated in Fig. 8 for the  $-\frac{1}{2} \rightarrow +\frac{1}{2}$  transition. The variation of this spectrum with  $\varphi$  is in first order of the form  $C_d a \cos[4(\varphi \pm \beta)]$ , where  $\varphi$  is the angle between  $H$  and the  $[100]$  direction. Note that this  $\varphi$  splitting is not observed for either octahedral or tetrahedral cases with  $H$  in a  $(110)$  plane; for  $H_1$  then makes the same angle  $\varphi = 60^\circ$  with the  $(a_1)$  and  $(a_2)$  sites and the same angle  $\varphi = 45^\circ$  for the  $(d_1)$  and  $(d_2)$  sites.  $C_d$  is found by first diagonalizing the Hamiltonian for  $\theta = 90^\circ$ , neglecting the  $e^{i4\varphi}$  terms, and using the values of  $D$  and  $(a + \frac{2}{3}F)$  determined from the parallel spectrum, with the appropriate signs as determined at low temperature. The diagonalization was done on a 704 computer. With the new wave functions  $\psi_i$ , the first order contribution,  $\langle \psi_i | a S_+^4 e^{i4(\varphi \pm \beta)} + \text{c.c.} | \psi_i \rangle$ , of the neglected terms to the energy of the  $S_z = \pm \frac{1}{2}$  levels are calculated, yielding an

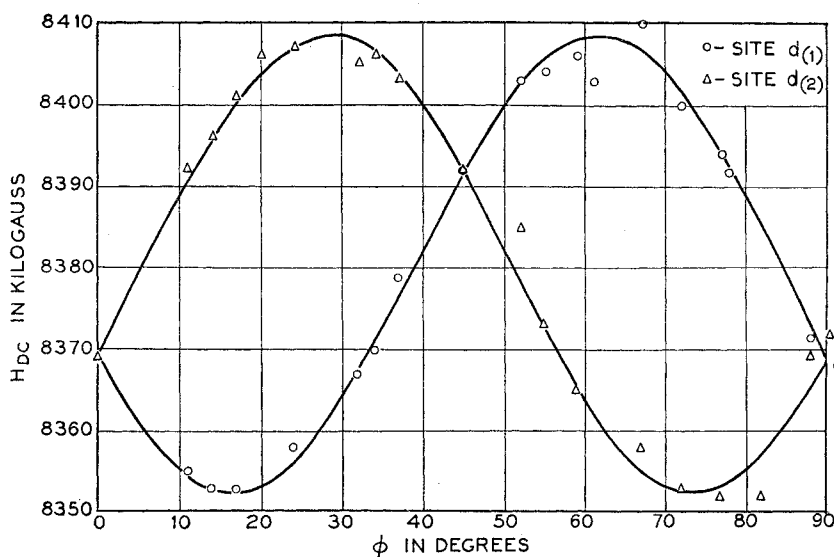


FIG. 8.  $\varphi$  splitting of the  $-\frac{1}{2} \rightarrow +\frac{1}{2}$  transition of  $\text{Fe}^{3+}$  in the tetrahedral site with  $H_{dc}$  rotated in a (001) plane.  $\theta = 90^\circ$ . The failure of some of the points to fall on the curve is due to the extreme pulling of these lines from the much stronger lines from the octahedral sites at certain angles.

additional term  $b \cos[4(\varphi \pm \beta)]$  in the energy difference ( $W_{+\frac{1}{2}} - W_{-\frac{1}{2}}$ ) for  $\theta = 90^\circ$ . With  $(W_{+\frac{1}{2}} - W_{-\frac{1}{2}})$  kept constant (fixed frequency experiment) this will correspond to a term  $C_d a_d \cos[4(\varphi \pm \beta)]$  in the field for resonance where  $C_d$  was found to be  $C_d = +0.426$ . Using this value of  $C_d$  and referring to the experimental results of Fig. 8,  $a$  including sign could be found if  $\beta$  were known, i.e., the position of the cubic crystalline field axes. These axes will, of course, coincide with the turning points of the spectra, but because of the two sites we cannot tell from the microwave measurements alone whether  $\beta = 16.5^\circ$  or  $28.5^\circ$ , and the two choices will give opposite signs for  $a$ . However, in the isostructural YIG,  $\beta$  was found to be  $15.6^\circ$  and we would expect it to be very much the same here so that we can rule out with certainty  $28.5^\circ$  and conclude therefore, that  $a$  is positive and equal to  $+0.0062 \text{ cm}^{-1}$ .

Turning to the octahedral site,  $a$  appears inde-

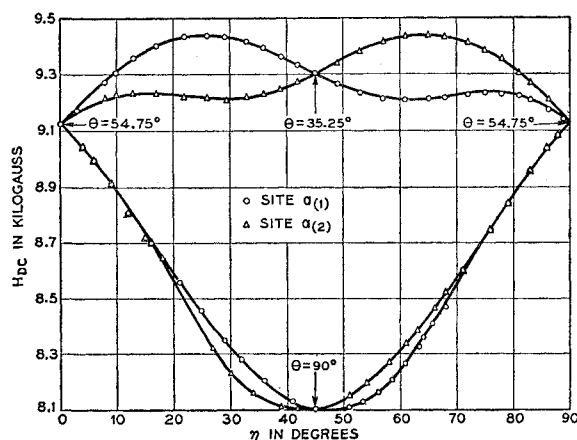


FIG. 9.  $\varphi$  splitting of the  $-\frac{1}{2} \rightarrow +\frac{1}{2}$  transition of  $\text{Fe}^{3+}$  in the octahedral site with  $H$  rotated in a (001) plane.  $\theta$  is not constant for the octahedral sites as  $H_{dc}$  is rotated in this plane.

pendently of  $F$  as an  $ae^{3i\varphi}$  term in the Hamiltonian of Eq. (3). If we again try to keep the axial terms constant and vary  $H$  azimuthally at  $\theta = 90^\circ$ , we find, however, no variation in the spectrum at all. This is due to the fact that the cubic anisotropy ( $S_x^4 + S_y^4 + S_z^4$ ) is constant in all directions at right angles to its threefold axes, i.e., in a plane perpendicular to the  $[111]$  direction. One could surmount this problem by keeping the field direction fixed and rotating the crystal about the  $c$  axis in such a way that this axis is always at a fixed angle to the field. In this way  $\theta$  could remain at a fixed angle to the field other than  $90^\circ$  and we would find an azimuthal variation in the spectrum.<sup>19</sup> However, to do this proved experimentally inconvenient, especially at low temperatures, and the following compromise was made. We studied the variation of the  $-\frac{1}{2} \rightarrow +\frac{1}{2}$  transition as  $H$  was rotated in the (001) plane with the experimental results indicated in Fig. 9. Starting at the  $[100]$  direction, all  $z$  axes of the octahedral sites make the same angle of  $\theta = 54.75^\circ$  with  $H$ . When  $H$  is rotated to a  $[110]$  direction,  $\eta = 45^\circ$ , the sites with their  $z$  axes along the  $[111]$  and  $[\bar{1}\bar{1}\bar{1}]$  will have  $\theta = 90^\circ$ , while those whose  $z$ -axes are along the  $[1\bar{1}1]$  and  $[11\bar{1}]$  directions will have  $\cos^{-1}\theta = (2/3)^{1/2}$ . Thus there is a large  $\theta$  variation in the spectra. However, there will be a further splitting on each  $\theta$  branch due to the two types of sites rotated from each other by  $2\alpha$  as shown schematically in Figs. 3 and 4. It was this  $\varphi$  splitting on the  $\theta = 54.75^\circ$  to the  $\theta = 35.25^\circ$  branch that was utilized to determine  $a$  similar to the procedure for the tetrahedral site, except that now the Hamiltonian had to be diagonalized at several values of  $\theta$ . This resulted in a perturbation of the form  $a_a C_a \cos[3(\varphi \pm \alpha)]$ , where now  $C_a$  was different for each  $\theta$ . The final result is  $|a_a| = 0.0185 \text{ cm}^{-1}$ . This value of  $|a_a|$  for octahedral oxygen coordination is comparable to the value found by Low<sup>5</sup> for  $\text{Fe}^{3+}$  in  $\text{MgO}$  and by

<sup>19</sup> E. Shulz-DuBois (private communication).



Müller<sup>20</sup> in  $\text{SrTiO}_3$ , but somewhat smaller than  $|a_a|$  in  $\text{Al}_2\text{O}_3$ .<sup>18,21</sup>

To find the sign of  $a_a$ , a knowledge of  $\alpha$  is required. If the angle  $\alpha$  were  $30^\circ$  then there would be no way *in principle* to determine the sign of  $a$ , as the two sites would be  $60^\circ$  apart and the  $e^{23(\varphi \pm \alpha)}$  term would simply introduce a sign change between the  $\varphi$  spectra of the two sites. Our experimental results indicate  $\alpha = 28^\circ$  or  $\alpha = 32^\circ$ . If we choose  $\alpha = 28^\circ$  on the basis that this is closer to the angle  $\alpha = 28.6^\circ$  found in YIG, we get a positive sign of  $a$ . One can look at this question the other way around and cite strong evidence from other directions to support a positive  $a$  and conclude *a posteriori* that  $\alpha = 28^\circ$ . This evidence comes from the positive  $a$  found by Low<sup>6</sup> for  $\text{Fe}^{3+}$  in similar octahedral oxygen coordination as well as the positive value of  $(a-F)$  found in this experiment. To assume a negative  $a$  would imply a value of  $F$  almost one-fourth as large as  $D$  which is highly unlikely as  $F$  is a fourth order term compared to  $D$  which is a second order term.

## V. DISCUSSION OF RESULTS

### 1. Relationship of Results to Crystal Field Theory

We wish to make here a few brief observations on the bearing of the experimental results for  $D$  and  $a$  upon the theory of the crystal field splitting of the ground state of  $S$ -state ions.

As pointed out in the introduction, Watanabe's theory of the splitting of  $S$ -state ions in cubic fields predicted that  $a \sim V^2$  ( $V$  is the cubic crystalline potential) if perturbations by states derived only from the  $3d^5$  configuration are considered. Perturbations from states derived from higher configurations such as  $3d^4s$  would give a contribution proportional to  $V$  but would be expected to be a few orders of magnitude smaller. This can be estimated as follows. Processes contributing to  $a$  involving terms of  $d^5$  only are of the order<sup>1</sup>

$$\lambda^4 V^2 / (\Delta E)^5, \quad (7)$$

where  $\lambda$  is the spin-orbit coupling constant,  $V$  is the cubic crystalline potential, and  $\Delta E$  is an average separation of the  $^6S$  ground state from the excited states in  $d^5$ . This is to be compared with processes linear in  $V$  which involve the excited configurations and which are of order<sup>22</sup>

$$\lambda^4 V / (\Delta \epsilon)^4, \quad (8)$$

where  $\Delta \epsilon$  is an average separation of the excited configurations (i.e.,  $3d^4d$ ) from the  $^6S$  ground state. Taking  $V \sim 10^4 \text{ cm}^{-1}$ ,  $\Delta E = 3 \times 10^4 \text{ cm}^{-1}$  and  $\Delta \epsilon \sim 10^5 \text{ cm}^{-1}$ , it is seen that perturbations from terms within  $d^5$  are about 100 times more effective.

Our experimental results have shown that  $a$  is positive for  $\text{Fe}^{3+}$  in both (a) and (d) sites even though the potentials are different in sign. As a matter of fact all the experimental data for  $^6S_5(3d^5)$  seems to indicate that  $a$  is always positive in both coordinations and for a variety of ligands, i.e., water, oxygen, sulfur, etc. We have previously shown that a negative  $a$  for  $\text{Fe}^{3+}$  in the alums was in error and that  $a$  is positive in these compounds as well.<sup>23</sup> This could have been inferred from the result of Bleaney and Trenam<sup>17</sup> that  $a$  and  $D$  for  $\text{Fe}^{3+}$  in methylamine sulfate had the same sign in conjunction with the data of Cooke, Meyer, and Wolf<sup>24</sup> who found  $D$  positive from specific heat measurements in ferric methyl ammonium sulfate. This might all be taken as support for that aspect of the theory which predicts  $a \sim V^2$ .<sup>25</sup>

However, Powell, Gabriel, and Johnston<sup>2</sup> have re-examined Watanabe's argument which led one to expect that only contributions even in  $V$  arise from terms in  $d^5$ . They point out that in going from a picture of electrons to one of holes the sign of  $\lambda$  as well as  $V$  changes so that one may have odd powers in  $V$  and  $\lambda$  simultaneously. This has also been shown by Lacroix<sup>26</sup> by the use of very general group theoretical methods. The calculation of Powell, Gabriel, and Johnston shows that indeed contributions odd in  $V$  arise from terms in  $d^5$ . A contribution of this nature, for example, would involve  $V$  to the first power and  $\lambda \cdot S$  to the fifth power. At first glance the appearance of the spin operator to the fifth power may seem awkward as we should like to derive a quartic spin Hamiltonian from this perturbation. However, assuming the correctness of their calculation implies of necessity that such a reduction from fifth powers of spin to fourth power by the use of the spin commutation relations must take place.

On the experimental side, the fact that  $a$  is invariably found to be positive, independent of the sign of  $V$ , must now be regarded as only establishing the *dominance* of terms even in  $V$ .<sup>27</sup> Their calculation is in agreement with this experimental fact, for even though  $a$  is not an even function of  $V$  it is nonetheless positive for both positive and negative  $V$  for reasonable values of  $V$ .

One might go even further and examine how the relative magnitudes of the  $a$ 's for the (a) and (d) sites compare with each other using a naive point-charge model. The constant  $C$  appearing in the cubic potential [Eq. (1)] is  $-(35/9)q/d^5$  and  $+(35/4)q/d^5$  for tetrahedral and octahedral sites, respectively, where  $d$  is

<sup>23</sup> S. Geschwind, Phys. Rev. Letters **3**, 207 (1959).

<sup>24</sup> A. H. Cooke, H. Meyer, and W. P. Wolf, Proc. Roy. Soc. (London) **A237**, 404 (1956).

<sup>25</sup> The author is indebted to Dr. H. Meyer and Dr. W. P. Wolf for pointing this out.

<sup>26</sup> R. Lacroix, Helv. Phys. Acta **30**, 478 (1957).

<sup>27</sup> A negative value of  $a \sim -1.0 \times 10^{-4} \text{ cm}^{-1}$  was needed by Watkins to explain the spectra of  $\text{Mn}^{2+}$  in NaCl; G. D. Watkins, Phys. Rev. **113**, 79 (1959). However, while such a small value of  $a$  is consistent with very small values of  $Dq$  in the table of reference 2, it could also arise from excited configurations.

<sup>20</sup> K. A. Müller, Helv. Phys. Acta **31**, 173 (1957).

<sup>21</sup> G. S. Bogel and H. F. Symmons, Proc. Phys. Soc. (London) **73**, 531 (1959).

<sup>22</sup> M. H. L. Pryce, Phys. Rev. **80**, 1107 (1950).

the distance from the center of the site to the charges  $q$  located at the corners. If  $a \sim V^2$ , then  $a_a/a_d = (9/4)^2(d_d/d_a)^{10}$ . Using the Fe—O distances given by Geller and Gilleo<sup>16</sup> for YIG,  $d_d = 1.88$  Å, and  $d_a = 2.00$  Å, one predicts  $a_a/a_d = 2.72 \pm 0.3$  the error arising from the uncertainty in  $d$ . This is in very good agreement with our experimental value  $3.00 \pm 0.1$  from Table I. While the point-charge model is an oversimplification it might have some validity in relative comparisons of this sort in cases where the bonding is fairly ionic, i.e., fluorine and oxygen coordination. One would not expect it to work in more covalent cases such as sulfur coordination.

Turning to the axial field splitting parameter,  $D$  is found to be positive for  $\text{Fe}^{3+}$  in  $\text{Al}_2\text{O}_3$ ,<sup>21</sup> while it is negative in YGaG for both sites. It is therefore apparent that terms linear in  $V_{\text{ax}}$ , in the axial field splitting of the ground state are effective and therefore the admixing of higher configurations is involved. This term could arise from a process proposed by Pryce<sup>22</sup> of the type

$$\frac{\langle {}^6S(3d^5) | V_{\text{ss}} | {}^6D(3d^44s) \rangle \langle {}^6D(3d^44s) | V_{\text{ax}} | {}^6S(3d^5) \rangle}{W({}^6S) - W({}^6D)}, \quad (9)$$

where  $V_{\text{ax}}$  is the axial crystal potential, and  $V_{\text{ss}}$  the spin-spin interaction energy. A calculation using a point charge model indeed shows opposite signs for  $V$  in  $\text{Al}_2\text{O}_3$  compared to YGaG. However, a closer examination of all the available experimental evidence on  $\text{Fe}^{3+}$ , which will be reported later, suggests that a small term quadratic in  $V$  may also be effective. This again can arise from terms of  $3d^5$  and is of the form, for example of<sup>1</sup>

$$\frac{\langle {}^6S | \lambda \mathbf{L} \cdot \mathbf{S} | {}^4P \rangle \langle {}^4P | V_{\text{ax}} | {}^4D \rangle \langle {}^4D | V_{\text{ax}} | {}^4P \rangle \langle {}^4P | \lambda \mathbf{L} \cdot \mathbf{S} | {}^6S \rangle}{[W({}^6S) - W({}^4P)][W({}^6S) - W({}^4D)][W({}^6S) - W({}^4P)]}, \quad (10)$$

If we take  $V_{\text{ax}} \sim 10^3 \text{ cm}^{-1}$  and  $V_{\text{ss}} \sim 1 \text{ cm}^{-1}$  and  $\lambda = 400 \text{ cm}^{-1}$ ,  $\Delta E = 3 \times 10^4 \text{ cm}^{-1}$ , and  $\Delta \epsilon = 10^5 \text{ cm}^{-1}$ , it is seen that Eq. (9) and Eq. (10) are the same order of magnitude so that unlike the case of the cubic potential, terms both linear and quadratic in  $V_{\text{ax}}$  may be expected to contribute almost equally to  $D$ .

These order of magnitude estimates are tendered with caution as a more detailed examination of the problem must consider overlap and covalent effects, for example, as indicated recently by Kondo.<sup>23</sup> A fuller summary of all the experimental data pertinent to the problem will appear in a forthcoming publication.

## 2. Anisotropy of YIG

The crystal field parameters  $a$ ,  $D$ ,  $F$  reflect the anisotropy energy of an individual isolated  $\text{Fe}^{3+}$  ion relative to the orientation of its spin with respect to the local crystal field axes. The "single ion" theory of ferromagnetic anisotropy proposes that in a ferrimagnet the

anisotropy energy is given by summing the individual anisotropy of each ion over all crystal sites. The spin orientation of the ion will be determined by the Weiss molecular field whose direction will be called  $Z$ , and which has direction cosines  $\alpha_1$ ,  $\alpha_2$ , and  $\alpha_3$  with respect to the unit cell edges. Let the direction cosines of the local cubic crystal field axes with respect to the Weiss field be  $n_1$ ,  $n_2$ , and  $n_3$  and let  $\theta$  be the angle between the Weiss field and the axial crystal field. Then the local anisotropy of an  $\text{Fe}^{3+}$  ion is given by

$$\begin{aligned} & \left[ \frac{1}{6}a(n_1^4 + n_2^4 + n_3^4) + (35/180)F \cos^4\theta \right] \\ & \times \left\{ \frac{1}{8}[35\langle S_z^4 \rangle - 30S(S+1)\langle S_z^2 \rangle \right. \\ & \left. + 3S^2(S+1)^2 - 6S(S+1) + 25\langle S_z^2 \rangle] \right\} \\ & + \left[ \frac{1}{2}D \cos^2\theta \right] \{ 3\langle S_z^2 \rangle - S(S+1) \}, \quad (11) \end{aligned}$$

where  $S_z$  is now the projection of  $S$  along the Weiss field and terms in  $\cos^2\theta$  multiplying  $F$  have been omitted as they do not contribute to the cubic anisotropy. This expression was derived for the  $a$  term by Yosida and Tachiki,<sup>8</sup> and an obvious extension of their method gives the  $F$  and  $D$  terms. Higher order terms in  $D^2/g\beta H_{\text{ex}}$  have been neglected as our result for  $D$  indicates they are less than  $10^{-4} \text{ cm}^{-1}$ . The terms in curly brackets are temperature factors calculated by Yosida and Tachiki<sup>8</sup> and Wolf.<sup>9</sup> In Wolf's notation the term in curled brackets containing  $S_z^4$  is equal to  $-3r(y)$ , where  $r(y) \rightarrow -\frac{5}{2}$  as  $T \rightarrow 0$  and  $r(y) \rightarrow 0$  as  $T$  approaches the Curie temperature. The term  $\cos^2\theta$  averaged over either the four different body diagonals or the three cube edges gives a constant term, so that in first order the term in  $D$  does not contribute to the cubic anisotropy. We are thus left with the terms in  $a$  and  $F$  where  $(n_1^4 + n_2^4 + n_3^4)$  and  $\cos^4\theta$  are to be averaged over the different sites whose crystal field axes are oriented differently with respect to the unit-cell axes.

In averaging the term  $(n_1^4 + n_2^4 + n_3^4)$  care must be taken in the selection of the local cubic axes for the distorted octahedra. As the distortion is along a  $[111]$  direction the cubic crystal field axes do *not* coincide with the body diagonals of the octahedron. Besides showing a threefold symmetry with respect to the direction of distortion, the cubic crystal field axes must be perpendicular to each other. This results in a slight alteration of Cooper's<sup>20</sup> result for this average but could be significant in cases of more severe distortions.

It is convenient to express this average in terms of the angles  $\alpha$  and  $\beta$  referred to earlier which measured the rotation away from coincidence with the unit cell edges of the cubic axes of the octahedral and tetrahedral sites respectively about their axes of distortion. If the anisotropy energy is expressed as  $K_1(\alpha_1^2\alpha_2^2 + \alpha_2^2\alpha_3^2 + \alpha_1^2\alpha_3^2)$ , then in terms of these angles the anisotropy constant *per unit cell* (24 tetrahedral plus 16 octahedral sites) becomes

$$K_1 = [a_d(14 + 10 \cos 4\beta) + (28/3)F_d]r_d(y) + [a_a(16/27)(7 + 20 \cos 3\alpha) - (112/27)F_a]r_a(y). \quad (12)$$

<sup>23</sup> J. Kondo, Progr. Theoret. Phys. (Kyoto) **23**, 106 (1960).

<sup>20</sup> B. R. Cooper, Phys. Rev. **112**, 395 (1959).

The angles  $\alpha$  and  $\beta$  are given in terms of the oxygen parameters  $x$ ,  $y$ , and  $z$  of the lattice by

$$\tan\alpha = \frac{1}{2}\sqrt{3}(y-x)/[z - \frac{1}{2}(x+y)], \quad (13)$$

$$\tan(\frac{1}{4}\pi - \beta) = y/(\frac{1}{4} - z). \quad (14)$$

The notation  $K_d$  and  $K_a$  is introduced for the coefficients of  $r_d(y)$  and  $r_a(y)$  in Eq. (12), i.e.,

$$K_1 = K_d r_d(y) + K_a r_a(y). \quad (15)$$

From the oxygen parameters of YIG given by Geller and Gilleo<sup>16</sup> it is found that  $\alpha = 28.6^\circ$  and  $\beta = 15.4^\circ$  which when substituted into Eq. (12) along with the values  $a$  and  $F$  from Table I yield the values  $K_d$  and  $K_a$  in column 1 of Table II.

Rodrigue, Meyer, and Jones<sup>30</sup> have used Pauthenet's<sup>31</sup> magnetization data for the ( $a$ ) and ( $d$ ) sublattices to determine  $r_d(y)$  and  $r_a(y)$  and have then fitted their measured anisotropy of YIG to Eq. (15) to determine the coefficient  $K_d(y)$  and  $K_a(y)$ .<sup>32</sup> Their results are listed in the second column of Table II where they are compared with the values of  $K_a$  and  $K_d$  calculated from the experimentally determined crystal field parameters of YGaG. While the values of  $K_d$  are in fair agreement it is seen that the values of  $K_a$  differ by about a factor of ten. Note also that the numerical result of this molecular field fit has been to place the burden of the anisotropy almost completely upon the tetrahedral sites. Even if one had misgivings about the applicability of molecular field theory here, one would at least hope for better agreement at  $T = 0^\circ\text{K}$ , where  $\langle S_z \rangle = \frac{5}{2}$  independent of any molecular field assumption so that  $r_d = r_a = -\frac{5}{2}$ . If  $r_d = r_a = -\frac{5}{2}$  is inserted in Eq. (12) we find  $K_1(T = 0^\circ\text{K}) = -0.37 \text{ cm}^{-1}$ , compared to the experimental value of  $K_1 = -0.241 \text{ cm}^{-1}$ .<sup>30</sup> Thus, we see that the experimental result for  $K_1$  of YIG differs by about 50% from that predicted theoretically when using the crystal field parameters  $a$  and  $F$  found for YGaG.

One is led to speculate about the source of the discrepancy.

(a) We initially look for an explanation within the framework of the "single ion" theory of anisotropy. Perhaps the parameters  $a$  and  $F$  are sufficiently different

in YIG compared to YGaG so that one is not justified in substituting the values of  $a$  and  $F$  determined in the magnetically dilute crystal. This suggestion is reasonable only in so far as  $F$  is concerned. In this connection, while no great variation is found in  $a$  for  $\text{Fe}^{3+}$  in octahedral oxygen coordination,  $F$  is very sensitive to the distortion of the octahedron.<sup>33</sup> One would need values of  $F$  almost three times larger than found here to explain the observed anisotropy of YIG. This may not be unreasonable, i.e.,  $\text{Fe}^{3+}$  in  $\text{Al}_2\text{O}_3$  has  $F \approx 100$  gauss.<sup>18,21</sup> Along this same line of thought, Kaminow<sup>34</sup> finds in his pressure experiments a 7% change in  $K_1$  in YIG for a one-half per cent change in volume. If we assume that the Fe—O distance follows the bulk volume compression then if  $a \sim V^{1/3}$  cubic, we expect  $\delta a/a = (\delta V/V)^{1/3}$ , which for a one-half percent volume change would only predict a change in  $K_1$  of 1.7%. Therefore, the larger percentage change in  $K_1$  that Kaminow observes probably reflects a change in  $F$ , more so than that of  $a$ , due to a change in the oxygen parameters, and further supports the expectation of significant variations in  $F$  between YIG and YGaG.<sup>35</sup>

(b) The cubic crystal field axes may not be given simply by the six nearest oxygen neighbors but next nearest neighbors may be playing a role. In this case, the angle  $\alpha$  in Eq. (12) would be further rotated. Note that an angle  $\alpha = 36.8^\circ$  will result in the vanishing of the contribution of  $a_a$  to the anisotropy. However, a simple point-charge calculation shows that this added rotation could not amount to more than one degree. In addition, this angle as determined from the paramagnetic resonance experiments in YGaG reflects the local cubic crystal field at the site due to all the remaining charges in the crystal. Again, it is difficult to see how this angle could vary as much as from  $28^\circ$  in YGaG to  $35^\circ$  in YIG, which is needed to explain the results.

(c) A small impurity may be contributing strongly to the anisotropy. Dillon has succeeded in modifying the anisotropy of YIG by incorporating fractional percentages of silicon into the lattice which presumably forces a corresponding amount of iron into the divalent state. However, the chief effect was to introduce higher anisotropy terms rather than severely modify  $K_1$ .<sup>36</sup>

We return now for an explanation of this discrepancy to processes which involve interactions between the spins.

(d) Walker<sup>37</sup> has made the suggestion that since the spins are really not aligned in the ground state of a ferrimagnet, the anisotropy will be substantially reduced below that of the aligned state. Preliminary calculations

TABLE II. Comparison of calculated anisotropy per unit cell of ( $a$ ) and ( $d$ ) sublattices of YIG using crystal field parameters of Table I, with values deduced from measured anisotropy and molecular field theory fit.

	Using $a$ and $F$ from Table I	Rodrigue, Meyer, and Jones <sup>30</sup>
$K_a$ (16 octahedral sites)	$66 \times 10^{-3} \text{ cm}^{-1}$	$-6.4 \times 10^{-3} \text{ cm}^{-1}$
$K_d$ (24 tetrahedral sites)	$82 \times 10^{-3} \text{ cm}^{-1}$	$101 \times 10^{-3} \text{ cm}^{-1}$

<sup>30</sup> G. P. Rodrigue, H. Meyer, and R. V. Jones, J. Appl. Phys. **31**, 376S (1960).

<sup>31</sup> R. Pauthenet, Ann. phys. **13**, 424 (1958).

<sup>32</sup> Previous attempts<sup>11, 8, 27</sup> to determine values of  $a$  in tetrahedral coordination, by fitting to the experimental anisotropy in ferrites and garnets have predicted the wrong sign of  $a$ .

<sup>33</sup> J. F. Dillon, Jr. (private communication).

<sup>34</sup> I. Kaminow, quoted in reference 30.

<sup>35</sup> Note added in proof. Folen has also cited evidence for a significant variation in the  $F$  parameter between the ordered and disordered state in lithium ferrite [V. J. Folen, J. Appl. Phys. **31**, 166S (1960)].

<sup>36</sup> J. F. Dillon, Jr. (private communication).

<sup>37</sup> L. R. Walker, J. Appl. Phys., **32**, Suppl. (1961).

by him indicate that this effect may in fact resolve the remaining discrepancy.

(e) Finally, since the disagreement with experiment is only 50%, one should perhaps reconsider refining the calculation of the dipole-dipole interaction which according to Yosida and Tachiki<sup>8</sup> gives in  $\text{MnFe}_2\text{O}_4$  a value of  $K_1$  approximately 10% of the observed anisotropy.

In conclusion although there is a 50% disagreement between the observed and calculated anisotropy of YIG at  $T=0^\circ\text{K}$ , using the crystal field parameters of YGaG, we feel that the major portion of the anisotropy in cubic ferrimagnets arises from the cubic crystal field

splittings and that the remaining discrepancy could be explained by any one or combination of items (a) to (e).

#### ACKNOWLEDGMENTS

The author should like to thank D. Linn for his experimental assistance throughout the course of this work; S. Geller for this extensive aid with the important crystallographic problems; J. P. Remeika and J. W. Nielsen for the difficult task of growing the garnet single crystals; K. D. Bowers, A. M. Clogston, J. F. Dillon, Jr., A. Javan, M. Peter, E. Schulz-DuBois, and L. R. Walker for the many helpful discussions and Miss B. Cetlin for her help with the computations on the IBM 704.

### Sputtering of Silicon with $\text{A}^{+2}$ Ions

S. P. WOLSKY AND E. J. ZDANUK

*Research Division, Raytheon Company, Waltham, Massachusetts*

(Received August 26, 1960)

A gravimetric technique involving a sensitive quartz microbalance was used for the determination of sputtering yields for the argon ion-bombardment of silicon. The sputtering yield for  $\text{A}^{+2}$  ions was deduced from the results of experiments in which the relative concentrations of  $\text{A}^+$  and  $\text{A}^{+2}$  ions were varied in a known manner. On the assumption that sputtering is a kinetic-energy-controlled phenomenon, we would expect  $S_E(\text{A}^{+2}) = S_{2E}(\text{A}^+)$ , where  $S$  is the number of atoms sputtered by an impinging ion of energy  $E$ . This investigation showed, however, that  $S_E(\text{A}^{+2}) \simeq 4S_{2E}(\text{A}^+)$ . This indicates the influence in the sputtering process of some other factor in addition to the ion kinetic energy.

**A**N investigation of the sputtering of silicon with argon ions has provided information of the relative effectiveness of singly and doubly charged ions in the sputtering process. The presence of doubly charged ions in the discharge used for sputtering measurements has been found to have caused an overestimation of low-energy sputtering yields.<sup>1</sup> In this work a gravimetric technique involving a sensitive quartz microbalance in ultrahigh vacuum was used for *in situ* measurement of sputtering yields. Weight changes of  $0.13 \mu\text{g}$  (equivalent to  $10^{15}$  silicon atoms) with a maximum deviation of  $\pm 0.06 \mu\text{g}$  were detectable. The vacuum microbalance apparatus and its application to sputtering studies has been described in other publications.<sup>2,3</sup> The experimental procedure consisted essentially of the measurement of a weight change produced by bombardment of a sample with ions extracted from a thermionically supported low pressure discharge. Argon pressures were  $5 \times 10^{-4}$  to  $10^{-3}$  mm Hg. Discharge conditions were such that the ion energies were well defined and ion incidence

was predominantly normal to the target surface. A plasma potential of  $-4$  volts (with respect to ground) has been determined from probe measurements.<sup>2</sup> Current densities of 1 to  $17 \mu\text{a}/\text{cm}^2$  were employed, with a total of  $10^{16}$  to  $10^{19}$  ions being involved in any one experiment. The samples were high-purity oxygen-free (111)-oriented single-crystal slices,  $0.05$ – $0.1$  mm thick, with total surface areas of  $7$ – $10 \text{ cm}^2$ .

Figure 1 presents the sputtering yield,  $[S/(1+\gamma^*)]$ , as a function of the sample voltage for the argon bombardment of silicon at three different discharge voltages (DV).  $S$  is the number of atoms sputtered per impinging ion, and  $\gamma^*$  is a generalized correction factor applied to the charge count to yield the number of ions actually involved in the bombardment. For discharges having only singly charged ions,  $\gamma^* = \gamma$ , the ordinary secondary emission coefficient. For discharges having multiple charged ions,  $\gamma^*$  will contain corrections due to the secondary emission coefficient of the various species and to the multiple charges on some of the ions. At DV=35–40, only  $\text{A}^+$  are present<sup>4</sup> and  $S/(1+\gamma^*) = S/(1+\gamma)$ . The true ion energies are equal to the sample voltage less the plasma potential. The most interesting feature of these data, as far as this discussion

<sup>1</sup> R. Stuart and G. Wehner, Phys. Rev. Letters 4, 409 (1960).

<sup>2</sup> S. P. Wolsky, Phys. Rev. 108, 1131 (1957).

<sup>3</sup> S. P. Wolsky and E. J. Zdanuk, Proceedings of the U. S. Army Signal Research and Development Laboratories Conference on Vacuum Microbalance Techniques, Fort Monmouth, New Jersey, January, 1960 (unpublished).

<sup>4</sup> W. Bleakney, Phys. Rev. 36, 1303 (1930).

FIG. 5. Spectra observed with the magnetic field along a  $[111]$  direction. There are two octahedral spectra, one corresponding to  $\theta=0^\circ$  and three coincident spectra at  $\theta=70.5^\circ$  corresponding to the angle between  $H_{dc}$  and the other three body diagonals.

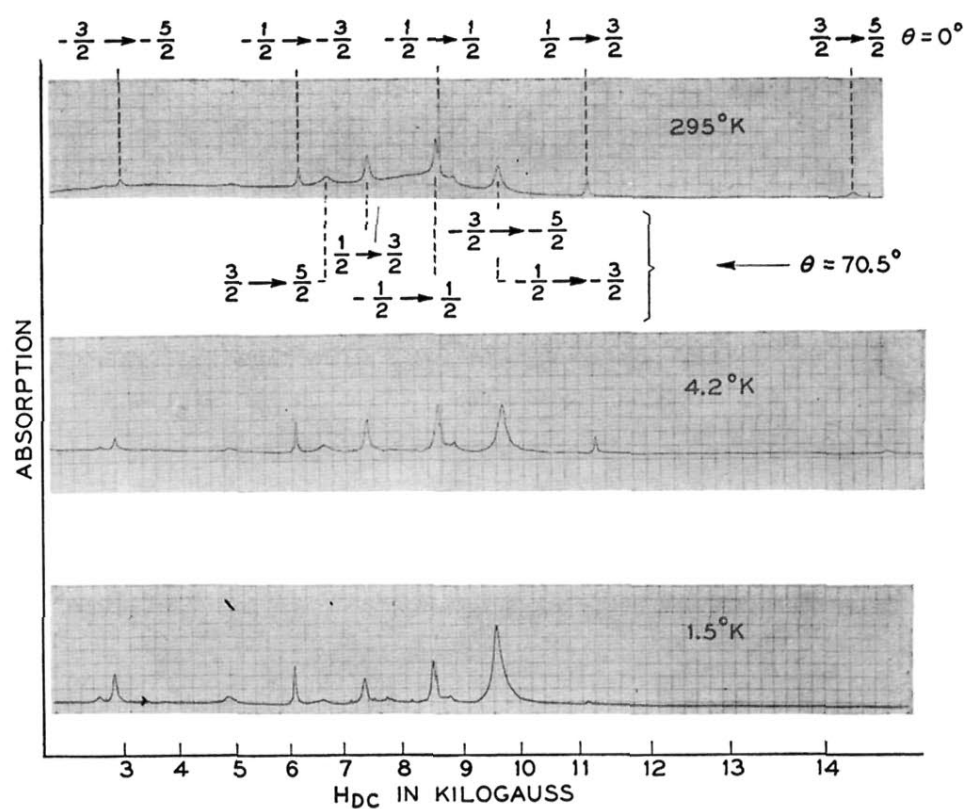


FIG. 7. Spectra observed with  $H$  along a  $[100]$  direction. The sharp line riding on the  $+\frac{1}{2} \rightarrow +\frac{3}{2}$  transition of the octahedral site is composed of two coincident  $-\frac{1}{2} \rightarrow +\frac{1}{2}$ ,  $\theta=90^\circ$  lines of the tetrahedral sites.

